Available online at www.sciencedirect.com

SciVerse ScienceDirect

Ceramics International 39 (2013) 4749–4756

CERAMICS INTERNATIONAL

www.elsevier.com/locate/ceramint

Influence of annealing on the structural, optical and photoluminescence properties of ZnO thin films for enhanced H_2 sensing application

K. Vijayalakshmi*, K. Karthick, D. Gopalakrishna

PG and Research Department of Physics, Bishop Heber College, Tiruchirappalli, Tamil Nadu, India

Received 6 October 2012; received in revised form 19 November 2012; accepted 20 November 2012
Available online 27 November 2012

Abstract

Nanostructured zinc oxide (ZnO) thin film sensors were prepared by spray pyrolysis, and their structural, optical, photoluminescence and morphological properties were investigated by X-ray diffractometer, UV–vis spectrometer, photoluminescence spectrometer, and scanning electron microscope (SEM), respectively. The post-annealing of ZnO film in air at 400 °C was found to be effective for the distribution of grains and their sizes, which favors the *c*-axis orientation of the film. This enhancement is accompanied by an increase in the optical band gap from 3.4 eV to 3.53 eV, which confirms the uniformity of ZnO film prepared by using a specially designed spray nozzle. SEM micrograph after heat treatment revealed uniform distribution of particles with well grown grains of ZnO. Hydrogen sensing measurement indicated the annealed ZnO film to show much higher response than the as deposited film. To understand the enhancement of the sensing performance of the annealed ZnO film, the gas sensing mechanism of the film was proposed and discussed. The magnitudes of the sensor response as well as its dependence on annealing differ significantly depending on the crystallite size of the film.

Keywords: C. Optical properties; ZnO thin films; Annealing; H_2 gas sensor

1. Introduction

One of the most critical needs in gas sensing is to develop low cost and portable hydrogen sensors that are able to selectively detect hydrogen gas near room temperature [1]. At present, commercial hydrogen detectors are not suitable for widespread use, as they are too bulky, expensive, and some are dangerous. The sensors working at high temperature themselves become a possible trigger of explosion due to the high input of electric energy for sensor operation. From the point of view of safety with the global environment, the present work has been realized with the necessity to develop hydrogen sensors working at low temperature. Recently, the main effort of H_2 sensor development has been the improvement of H_2 gas sensitivity as well as selectivity, and to decrease the operating temperature. Semiconducting metal oxide sensors, due to their small dimensions, low cost and high compatibility with microelectronic processing, have been widely investigated to meet the requirement of H_2 detection. Among various kinds of semiconducting metal oxide materials, zinc oxide (ZnO) is one of the pioneers and most promising H_2 sensing materials, due to its high chemical stability and easy fabrication [2,3].

ZnO is an n-type semiconductor of wurtzite structure with a large band gap energy of 3.37 eV at low temperature, and 3.3 eV at room temperature [4,5]. Its usefulness as a hydrogen sensor material was first realized after Seiyama et al. [6] demonstrated the detection of inflammable town gases by ZnO film. The physical properties of ZnO depend on the microstructure of the material, including crystal size, morphology, orientation, aspect ratio and crystalline density [7]. Sensing properties of ZnO are directly related to its preparation history, particle size, morphology and operating temperature. Many different methods such as RF/DC sputtering [8,9], sol–gel [10], metal organic chemical vapor deposition [11], and pulsed laser deposition [12] were used for the preparation of ZnO films. The spray pyrolysis technique was used extensively in

*Corresponding author. Tel.: +91 9994647287 (mobile).
E-mail address: viji71naveen@yahoo.com (K. Vijayalakshmi).

0272-8842/$ - see front matter © 2012 Elsevier Ltd and Techna Group S.r.l. All rights reserved.
http://dx.doi.org/10.1016/j.ceramint.2012.11.061

depositing metal oxide films [13]. The technique has excellent features such as being easy, low cost and simple, as no sophisticated equipment is required. The film produced with spray pyrolysis is inherently uniform and the surface to volume ratio of the nano drops is very large, making them very receptive to heat treatment and pyrolysis [14]. The film thickness and stoichometry are easy to control in this technique, and the resulting film is well compacted [15]. In the present work, the ZnO films were deposited by spray pyrolysis on a glass substrate kept at a temperature of 300 °C, and subsequently annealed at 400 °C for 1 h. The effect of annealing on the structural, morphological, optical, photoluminescence and H_2 sensing properties of the film was investigated.

2. Experimental details

ZnO thin films were deposited onto the glass substrate using 0.1 M concentration of aqueous solution of zinc acetate. To prepare 100 ml precursor solution, the required quantity of salt is dissolved in double distilled water. Before deposition, the substrates were cleaned in chromic acid and potassium dichromate in a liter of concentrated sulfuric acid. During synthesis, various preparative parameters like solution spray rate, nozzle to substrate distance, carrier gas flow rate, etc. were optimized in order to obtain transparent, uniform, adherent and pinhole free deposits. The deposition parameters used for the preparation of ZnO thin films in the present study are summarized in Table 1. Compressed air was used to atomize the solution containing the precursor compounds through a spray nozzle over the preheated substrate. The substrate holder was equipped with a thermocouple, heating element and a temperature controller. The spray nozzle is specially designed with two concentric glass pipes. Through the inner pipe flows the solution and between the inner and outer, the air stream; the spray was produced by the Ventury effect at the end of both pipes. Hazardous fumes evolving at the time of deposition were sucked out using an external exhaust system connected to the deposition chamber. The schematic diagram of the spray pyrolysis unit is shown in Fig. 1.

Table 1
Summary of deposition parameters for ZnO thin films.

Parameter	Values
Substrate temperature	300 °C
Solution feeding rate	3 ml/min
Carrier gas flow rate	0.4 kg/cm^2
Precursor concentration	0.1 M
Precursor Volume	100 M
Solvent	Water
Nozzle to substrate distance	30 cm
Deposition time	10 min
Temperature of annealing	400 °C

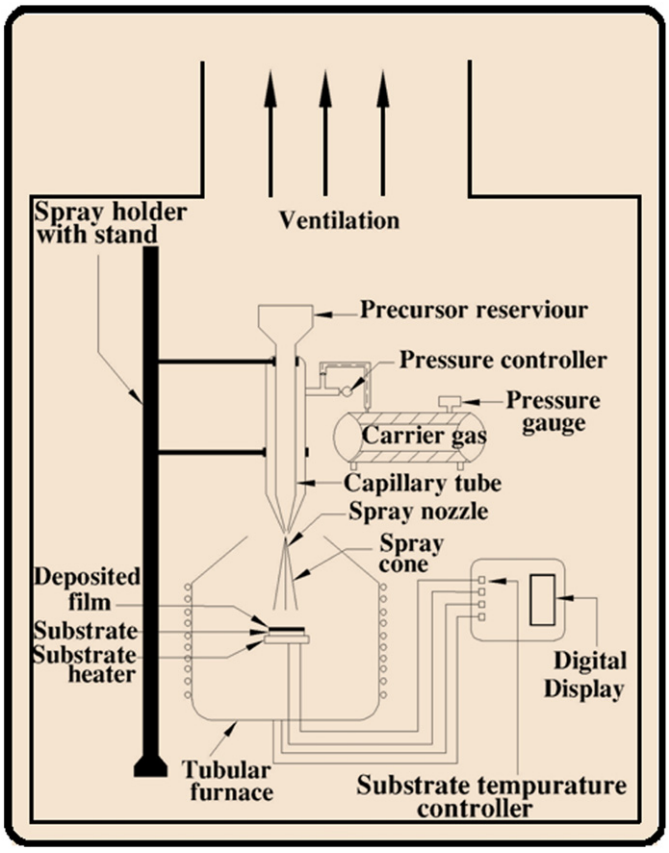

Fig. 1. Schematic of the experimental setup used for the spray pyrolysis deposition technique.

When the aqueous solution of zinc acetate was sprayed over the hot substrate, fine droplets of solution thermally decomposed after falling over the hot surface of the substrate. This resulted in the formation of a well adherent and uniform ZnO film. Rapid thermal annealing for 1 h at 400 °C after deposition determined desorption of the large number of chemisorbed oxygen species at the surface of freshly prepared ZnO film. The loss of adsorbed oxygen increased the electrons concentration of the surface and improved the conductance. These films were further used to investigate the structural, optical and photoluminescence properties. The structural characterization was carried out using an X Perto X-ray diffractometer with CuKα radiation, and optical characterization using a UV–vis Lambda-35 Spectrophotometer over the wavelength range 350–850 nm. Photoluminescence (PL) studies were carried out using a Varian Carry Eclipse PL spectrophotometer. The morphology of the films was studied using a HITACHI scanning electron microscope. The ZnO films prepared under the best deposition conditions found were used to fabricate a gas sensor in the desired geometry with two thick gold pads on two ends of the film to take out electrical contacts. Fig. 2 shows the schematic diagram of the experimental setup used for measuring the sensor resistivity. The ZnO sensor mounted on a Pt-heater was housed within an airtight chamber, with gas inlet and

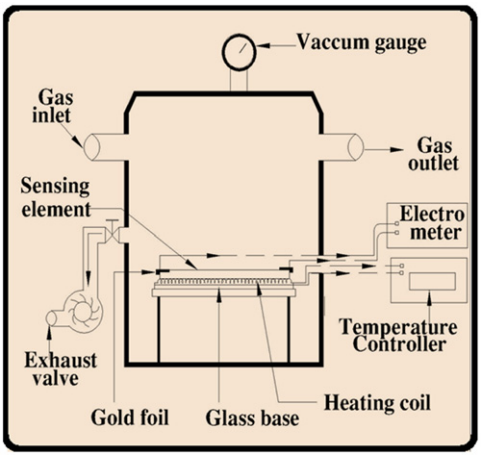

Fig. 2. Schematic of the experimental setup used for gas sensing measurement.

outlet valves. The sensor temperature was measured by the Ni–Cr thermocouple, with an accuracy of ± 1 °C using a temperature controller. The test gas diluted in air was admitted inside the chamber using mass flow controllers. An electric fan was installed in the container, which improve uniformity of the gas and flow of air. The resistance of the sensor was measured for different temperatures in gas–air ambient. The response of the sensor for reducing gases was defined as [16], $S = R_a - R_g/R_g$, where R_g and R_a are the electrical resistance of the sensor in the presence of test gas and in air, respectively.

3. Results and discussion

3.1. Effect of annealing on the structure and orientation of the ZnO film

The X-ray diffraction patterns of the as deposited and annealed ZnO films are shown in the Fig. 3(a) and (b), respectively. All diffraction peaks are indexed with JCPDS card file [6-4016]. The pattern confirmed that the ZnO films were polycrystalline in nature and belong to the hexagonal wurtzite structure of ZnO. The prepared ZnO film was very thin with no preferential orientation. The pattern shows [1 0 0], [0 0 2], [1 0 1] and [1 0 3] reflections. After annealing crystallinity of the film was found to increase, and the intensity of [002] peak improved dramatically, while the intensity of [100] and [101] reflection decreased. The results show that annealing favors the diffusion of atoms absorbed on the substrate and accelerates the migration of atoms to the energy favorable positions, crystallinity and the *c*-axis orientation of film, which is indicated by the increase in intensity of [002] reflections and decrease of full width at half maximum value [FWHM]. The crystalline size (D) was calculated by using the well-known Debye–Scherrer's formula [17]

$$D = k\lambda/\beta\cos\theta \quad (1)$$

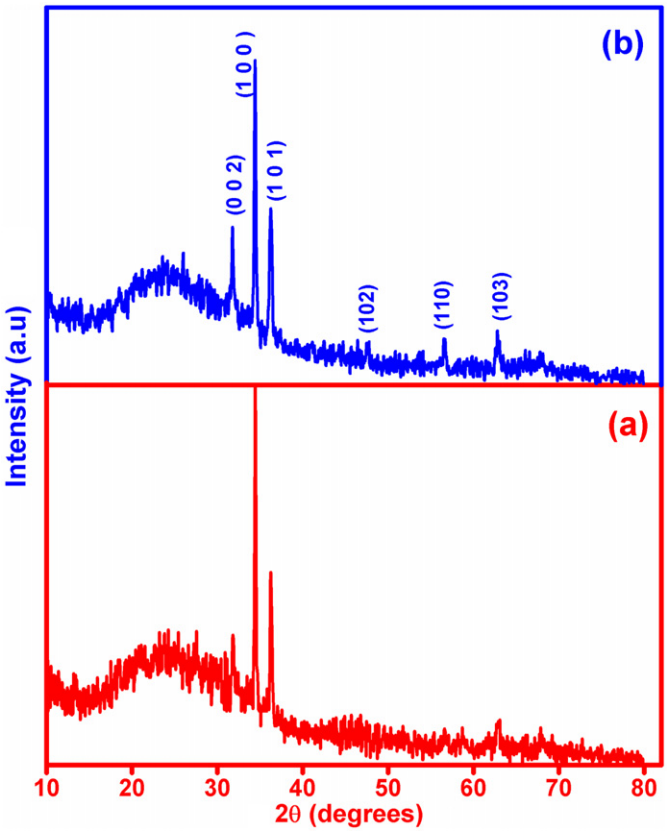

Fig. 3. X-ray diffraction patterns of the ZnO film prepared at 300 °C: (a) as deposited and (b) annealed at 400 °C.

where, k is a constant taken to be 0.9, λ is the wavelength of the incident X-ray ($\lambda = 1.5418\pi^{\circ}$), β is the corrected FWHM for instrument broadening of the maximum intensity peak, and θ is the angle at which the maximum peak occurs. The average crystallite size of the film was found to be ~44 nm for the [002] plane, which increased to 52 nm with annealing. The crystal defect parameters like microstrain and number of crystallites are calculated using the formula [18]:

$$\varepsilon = \beta Cos\theta/4 \quad (2)$$

$$N = t/D^3 \quad (3)$$

where ε is the microstrain of the film, N is the number of crystallites, and t is the thickness of the film. The measured crystallite size, microstrain and interplanar spacing of the ZnO film before and after annealing are reported in Table 2. It is clear from the table that the structural parameters are temperature dependent due to the expansion of the lattice with annealing. A slight change in the diffraction angle and corresponding d value of the lattice spacing of the preferential orientation of the films, before and after annealing, gives the evidences of the strain in the ZnO films. However, it can also be seen that the fundamental effect of increase in crystallite size after annealing is related to the decrease in strain. The decrease in strain

Table 2
Structural parameters of as the deposited and annealed ZnO films.

Stage	Diffraction angle 2θ (deg.)	(*hkl*)	d_{hkl} (Å)		Crystallite size (nm)	Microstrain $\times 10^{-3}$	No. of crystallites $\times 10^{16}$
			Reported	Calculated			
As deposited	31.7671	100	2.8145	2.8121	21.96	1.6505	2.9281
	34.4156	002	2.6037	2.5850	44.16	0.8209	0.3603
Annealed	36.2288	101	2.4775	2.4722	33.98	1.0666	0.7907
	31.8260	100	2.8118	2.8121	29.27	1.2387	2.7207
	34.4226	002	2.6032	2.5850	52.21	0.5740	0.3982
	36.2534	101	2.4759	2.4722	44.40	0.8164	0.6475

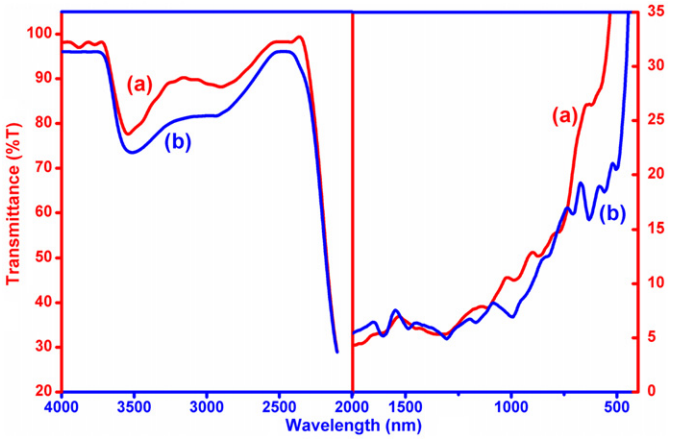

Fig. 4. FTIR spectra of ZnO film: (a) as-deposited and (b) annealed at 400 °C.

indicates the decrease in concentration of the lattice imperfections, and formation of high quality film.

Infrared transmittance spectra were employed to study the vibration bands for ZnO thin films, and changes due to annealing were contrasted to that as deposited. Fourier transform infrared (FTIR) spectra were recorded in the range of 400–4000 cm^{-1} for as deposited and annealed ZnO films, and it is shown in Fig. 4. The position and number of absorption bands not only depend on crystal structure and chemical composition, but also on the particle morphology. The ZnO spectra showed a large absorption band at $\sim$3544 cm^{-1}, characteristic of OH stretching vibration. The peaks around 1615 cm^{-1} were thought as the asymmetrical stretching vibration of C=O mode of zinc mono acetate [19]. The peak near 2903 cm^{-1} was due to the existence of asymmetrical and symmetrical CH bonds in the reaction between mono-acetate and water. Other absorption bands at $\sim$1347, $\sim$1615 and $\sim$1822 cm^{-1} were assigned to the bend deformation of water. The absorption band at $\sim$600 cm^{-1} was due to metal oxide bonds [20]. FTIR spectra of the annealed sample reveal that the most prominent absorption bands around $\sim$660 cm^{-1} were a clear evidence for the presence of crystalline ZnO. The peaks around 1347 cm^{-1} disappear after annealing, which mainly results from the decomposition of zinc acetate [20].

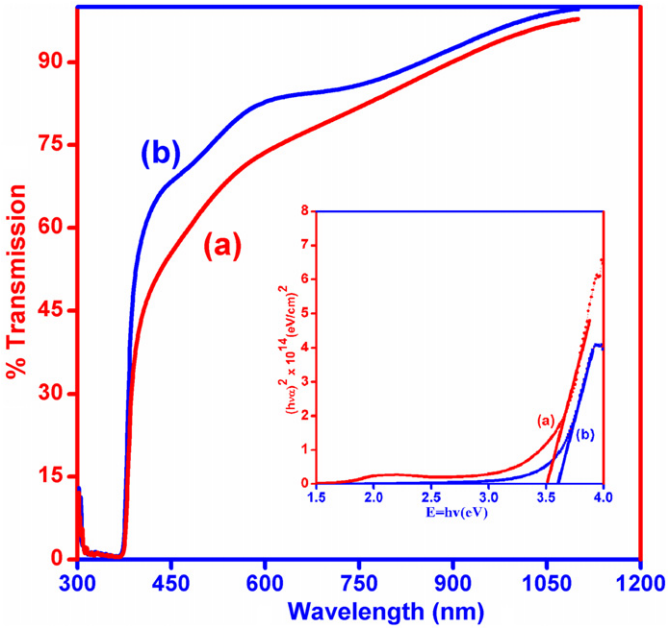

Fig. 5. Optical absorption spectra of ZnO film: (a) as-deposited and (b) annealed at 400 °C.

3.2. *Effect of annealing on the optical and photoluminescence properties of ZnO film*

The optical transmission spectra of both as deposited and annealed ZnO films were recorded as a function of wavelength in the range 350–900 nm, and are shown in Fig. 5. The optical absorption or absorption edge corresponds to the transition from valence band to conduction band, while the absorption in the visible region was related to some local energy levels caused by some intrinsic defects. The well developed interference pattern in transmittance spectra revealed that the films were specular to a great extent. The transmittance of the as deposited film was found to be 86% in the visible range, and it improved to 90% after annealing. The relatively low value of the transmittance of the as deposited film is attributed to scattering and absorption. The scattering resulted from the existence of grain boundaries, the point defect and the disorder of ZnO film. Moreover, the increase in the transmittance of the sample after annealing at 400 °C, is

attributed to the removal of organic species on the film, which show uniform, well adherent and highly crystalline films, as revealed from the XRD results. The band gap of the film was calculated using the Tauc relationship [21]

$$\alpha h\upsilon = A\left(h\upsilon - E_g\right)^n \quad (4)$$

where α is the absorption coefficient, A is a constant, h Plank constant, υ the photon frequency, E_g the energy band gap and n is 2 for the indirect band gap semiconductor. The inset of Fig. 5 shows the plot of $(\alpha h\upsilon)^2$ vs. $h\upsilon$. Extrapolation of the linear portion of the graph to $h\upsilon$ axis gives the band gap of the film. The band gap was found to be 3.46 eV and 3.52 eV for the ZnO film before and after annealing, respectively. The increase in band gap is attributed to the evaporation of impurity ions (OH^-), which causes a lowering of the band gap. Moreover, a high value of band gap after annealing confirms the surface smoothness and uniformity of ZnO films prepared under the optimized spray condition.

A study of the photoluminescence property of ZnO is very important because it can provide more valuable information on the quality and purity of the material. Fig. 6(a) and (b) shows the PL spectra of as deposited and annealed ZnO film, respectively. A strong and sharp UV emission peak centered at 373 nm, and a weak blue emission at 442 nm were obtained for the prepared ZnO film. Eun Sub Shim et al. [22] have reported that the intensity of UV emission of ZnO films may be due to the excitonic related recombination, dependent on the microcrystalline structure and stoichiometry of the film. It is well known that bulk ZnO cannot emit light at room temperature. However, PL emissions of our nanocrystalline ZnO samples were possibly due to the effect of oxygen vacancies. The oxygen vacancies would be generated due to the partial or incomplete oxidation of the precursor. The oxygen vacancies would generally act as deep donors and cause the formation of a new energy level in the band gap of ZnO nanoparticles, which results from radiative recombination of an electron occupying oxygen vacancies with a photo-excited hole [23]. Post-growth annealing could improve the emission efficiency due to the decrease of the nonradiative defects and the increases of ZnO grain size. As expected, the emission intensity increases and peak position shifts to the short wavelength with annealing (Fig. 6(b)). The shift in the peak is due to complete factors involving band gap shift, as well as the change in nanoparticle size [24], as revealed from the XRD results.

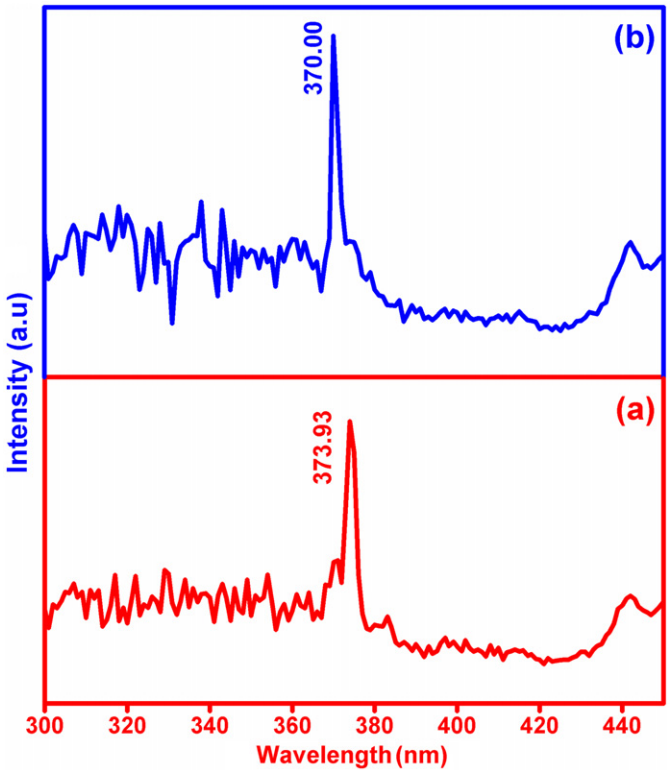

Fig. 6. PL spectra of ZnO film: (a) as- deposited and (b) annealed at 400 °C.

3.3. Effect of annealing on the morphological properties of ZnO films

Scanning electron microscopy was used to study the morphology of the film. Fig. 7(a) and (b) shows the SEM micrographs of as deposited and annealed ZnO films, respectively. The micrograph of the as deposited film displays fine and uniform distribution of particles throughout the surface. From the micrographs, it is clearly observed that the films are porous, indicating the suitability of ZnO films for gas sensing applications. After annealing, the film revealed a significant change in the morphology. The annealed film contained tightly packed nanoparticulates free of microcracks. The effect of annealing improved the structural homogeneity and the degree of crystallinity of the film. Zhu et al. [25] reported that the low temperature (200–450 °C) annealing treatment has no effect on the SEM images, but our results showed a remarkable change in the morphology of the film even at 400 °C. The average grain size of the film observed from SEM image is in good agreement with the average crystallite size calculated from XRD measurement.

3.4. Gas sensing properties of ZnO films

Fig. 8(a) and (b) shows the response of as deposited and annealed ZnO sensors with operating temperature toward 500 ppm H_2, respectively. The sensor response for the as deposited and annealed ZnO films went through a maximum at 100 °C and then decreased. The sensing mechanism for H_2 at room temperature can be represented by the following reaction [2]:

$$O^- + 2H \rightarrow H_2O + e^- \quad (5)$$

$$2H2 + O^- \rightarrow 2H_2O + e \quad (6)$$

On the sensor surface, the hydrogen gas splits up into hydrogen atoms, which forms protons by donating the

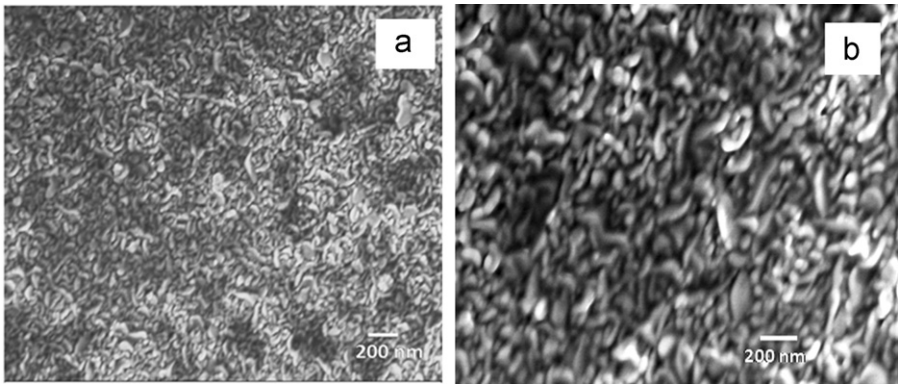

Fig. 7. SEM images of ZnO film: (a) as-deposited and (b) annealed at 400 °C.

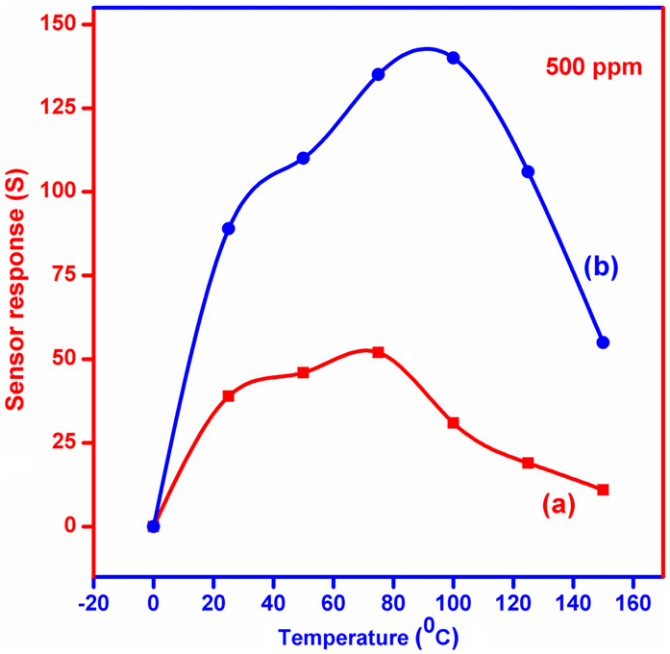

Fig. 8. The variation in sensor response of ZnO with operating temperature, upon exposure to 500 ppm H_2. (a) as-deposited and (b) annealed at 400 °C

electrons to the conduction band of ZnO film. The electron gain increases the film conductivity, which is reflected by a hump in the response at 100 °C. The generated proton gets associated with the surface adsorbed oxygen ions (O_2^- or O^- ions), and hops from one oxygen ion to another. During this process, the two adjacent OH^- groups may condense to form H_2O. On the other hand, the gas sensing response of ZnO sensors has been shown to be influenced by many extrinsic factors which include crystallite size and microstructure. The crystallite size of ZnO calculated from XRD measurement ranges from 20 to 40 nm in mean diameter, so that the sensing body includes pores called mesopores. Gas transport through mesopores is known to take place by Knudsen diffusion, the diffusion coefficient of which is given by [26]

$$D_k = 4r/3\left(2RT/I\pi M\right)^{1/2} \quad (7)$$

where r is the pore radius, M the molecular weight of target gas, R the gas constant and T the temperature. It follows that D_k is proportional to r, which would depend on the crystallite size of oxide used. The annealed ZnO sensor which contains large crystallites with well defined microstructure and uniform morphology, revealed a large response since r and D_k would tend to increase with increase in crystallite size. According to the reaction diffusion equation based analysis, the height of the response increases as observed in Fig. 8(b). It is suggested that this tendency mainly reflects an increasing order of the mesopores size or the Knudsen diffusion coefficient (D_k) involved among the films. Moreover, the higher response for the annealed ZnO film sensor relative to that of the as deposited one, indicate the consumption of large number of surface adsorbed oxygen ions (O_2, O, O^- ions) by H_2. The maximum sensor response is 62 for as deposited ZnO film to 500 ppm of H_2. The gas response increased to about 140 for the annealed ZnO film measured under the same condition. Several ZnO nano-thin film hydrogen sensors have been reported. The ZnO sensor prepared by RF sputtering revealed a sensitivity of 5 at 500 ppm H_2 in N_2 [27]. Furthermore, sensor based on ZnO multiple nanowires and exposed under 1000 ppm H_2 in N_2 at 150 °C, showed a high sensitivity of 43 [28]. By comparison, our annealed ZnO nanofilm sensor prepared by cost effective spray pyrolysis with specially designed nozzle structure, when exposed to 500 ppm H_2 showed a relative response of 140. The response of our sensor is attractive for further investigation of single ZnO nanostructures for practical H_2 sensor applications. These experimental results ensure the application of our novel sensor to detect H_2 at a low ppm range (1–1000 ppm) at room temperature.

Fig. 9(a) and (b) shows the variation in sensor response of as deposited and annealed ZnO films to various concentrations of H_2 at 100 °C, respectively. It is clear from the graph that the gas response goes on increasing

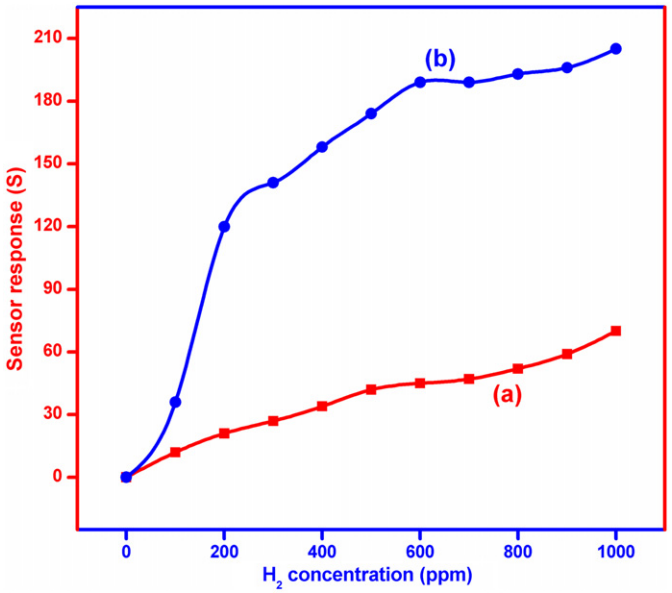

Fig. 9. The variation in sensor response of ZnO, upon exposure to various concentrations of H_2 at 100 °C: (a) as-deposited and (b) annealed at 400 °C.

linearly with gas concentration up to 500 ppm and gets saturated beyond it. The ratio of increase in gas response was relatively large upto 500 ppm. This is due to the fact that the monolayer of gas molecules formed on the surface would cover the whole surface of the film [2]. The gas molecules from that layer would reach the active site of the film. The excess gas molecules would remain idle and would not reach the surface active sites of the sensor. So the gas response at higher concentration of the gas is not expected to increase further to a large extent. Thus the active region of the sensor would be up to 500 ppm. The higher response for annealed ZnO relative to the as deposited film may be attributed to the large grain size of the film, which would be the optimum to get critical porosity. This in turn, would have favored and enhanced the gas response of the film.

4. Conclusion

ZnO thin films were deposited using a spray pyrolysis unit, with a specially designed spray nozzle at a substrate temperature of 300 °C, and subsequently annealed at 400 °C. The effect of annealing on the structural, optical, morphological and sensing properties of H_2 was investigated systematically. The results show that the crystalline quality and optical property of the ZnO film can be improved by annealing at 400 °C. SEM micrographs revealed that the morphology is significantly improved after heat treatment. The ZnO film responded very sharply and sensitively to H_2 in air at lower optimized temperature (25–120 °C). The magnitude of sensor response tended to increase as the crystallite size of annealed ZnO increased, suggesting the contribution by an increase in the mesopore size.

Acknowledgments

This work was financially supported by the University Grants Commission (MRP: 40-441/2011), which is gratefully acknowledged.

References

[1] G. Murugananthan, K. Ravichandran, K. Saravanakumar, A.T. Ravichandran, B. Sakthivel, Effect of solvent volume on the physical properties of undoped and fluorine doped tin oxide films deposited using a low-cost spray technique, Superlattices and Microstructures 50 (2011) 722–733.
[2] B. Subramanian, V. Swaminathan, M. Jayachandran, Micro-structural and optical properties of reactive magnetron sputtered Aluminum nitride (AlN) nano structured thin films, Current Applied Physics 11 (2011) 43–49.
[3] K. Saravanakumar, B. Sakthivel, K. Ravichandran, Simultaneous doping of aluminum and fluorine on zinc oxide nanopowder using a low-cost soft chemical route, Materials Letters 31 (2011) 2278–2280.
[4] V. Aroutiounian, Metal oxide hydrogen, oxygen and carbon monoxide sensors for hydrogen setups and cells, International Journal of Hydrogen Energy 32 (2007) 1145–1158.
[5] W.F. Liu, J.M. Bian, L.Z. Hu, H.W. Liang, H.Q. Zang, J.C. Sun, Z.W. Zhao, A.M. Liu, G.T. Du, Electroluminescence from a ZnO homojunction device grown by pulsed laser deposition, Solid State Communications 142 (2007) 655–658.
[6] T. Seiyama, A. Kato, K. Fulishi, M. Nagatani, A new detector for gaseous components using semiconductive thin films, Analytical Chemistry 34 (1962) 1502–1503.
[7] S. Badadhe, I.S. Mulla, Effect of aluminium doping on structural and gas sensing properties of zinc oxide thin films deposited by spray pyrolysis, Sensors and Actuators B—Chemicals. 156 (2011) 943–948.
[8] Li-Jian Bie, Xiao-Na Yan, Jing Yin, Yue-Qin Duan, Zhi-Hao Yuan, Nanopillar ZnO gas sensor for hydrogen and ethanol, Sensorsand Actuators B—chemicals. 126 (2007) 604–608.
[9] M. Suchea, S. Christolulakis, K. Moschovis, N. Katsarakis, G. Kiriakidis, ZnO transparent thin films for gas sensor applications, Thin Solid Films 515 (2006) 551–554.
[10] Ziaul Raza Khan, Mohd Shoeb Khan, Mohammad Zulfequar, Mohd Shahid Khan, Optical and structural properties of ZnO thin films fabricated by sol–gel method, Materials and Science and Applications 2 (2011) 340–345.
[11] Afishah Alias, Kouta Hazawa, Nobukai Kawashima, Hisashi Fukuda, Katushiro Uesugi, Fabrication of ZnO thin-film transistors by chemical vapor deposition method using zinc acetate solution, Japanese Journal of Applied Physics 50 (2011) 1–4.
[12] G. Epurescu, N.D. Scarisoreanu, D.G. Matei, G. Dinescu, C. Ghica, L.C. Nistor, M. Dinescu, Functional Zno thin films obtained by radiofrequency beam assisted pulsed laser deposition, Romanian Reports in Physics 60 (3) (2008) 807–814.
[13] Lou Xiao-Bo, Shen Hong-Lie, Zhang Hui, Li Bin-Bin, Optical properties of nanosized ZnO films prepared by sol-gel process,, Transactions.of Nonferrous Metals Society of China 17 (2007) 814–817.
[14] M.T. Mohammad, A.A. Hashim, M.H. Al-Maamory, Highly conductive and transparent ZnO thin films prepared by spray pyrolysis technique, Materials Chemistry and Physics 99 (2006) 382.
[15] Dainius Perednis, J. Gaukler, Thin film deposition using spray pyrolysis, Journal of Electroceramics 14 (2006) 103–111.
[16] P.P. Sahay, R.K. Nath, Al-doped zinc oxide thin films for liquid petroleum gas (LPG) sensors, Sensors Actuators B—Chemicals 133 (2008) 222–227.
[17] C.S. Prajapati, P.P. Sahay, Alcohol-sensing characteristics of spray deposited ZnO nano-particle thin films, Sensors Actuators, B—Chemicals 160 (2011) 1043–1049.

[18] P. Kathirvel, D. Manoharan, S.M. Mohan, S. Kumar, Spectral investigations of chemical bath deposited zinc oxide thin films—ammonia gas sensor, Journal of Optoelectronic and Biomedical Materials 1 (2009) 25–33.

[19] A.E. Jimenez-Gonzalez, Jose A. Soto Urueta, R. Suarez-Parra, Optical and electrical characteristics of aluminum-doped ZnO thin films prepared by solgel technique, Journalof Crystal Growth 192 (1998) 430–438.

[20] J. Coates, in: R.A. Meyers (Ed.), Interpretation of Infrared Spectra, A Partical Approach in Encyclopedia of Analytical Chemistry, John Willey & Sons Ltd., Chichester, 2000 pp.0815-10837.

[21] J. Tauc, R. Grigorovici, A. Vancu, Optical properties and electronic structure of amorphous germanium, Physica Status Solidi A 15 (1966) 627.

[22] Eun Sub Shim, Hong Seong Kang, Seong Sik Pang, Jeong Seok Kang, Ilgu Yun, Sang Yeol Lee, Annealing effect on the structural and optical properties of ZnO thin film on InP, Materials Science and Engineering B 102 (2003) 366–369.

[23] D. Geetha, T. Thilagavathi, Hydrothermal synthesis of nano Zno structures from Ctab, Digest Journals of Nanomaterials and Biostructures 5 (1) (2010) 297.

[24] Xiang Liu, Xiaohua Wu, Hui Cao, R.P.H. Chang, Growth mechanism and properties of ZnO nanorods synthesized by plasma-enhanced chemical vapor deposition, Journal of Applied Physics 95 (6) (2004) 3141–3147.

[25] B.L. Zhu, X.Z. Zhao, F.H. Su, G.H. Li, X.G. Wu, J. Wu, R. Wu, Low temperature annealing effects on the structure and optical properties of ZnO films grown by pulsed laser deposition, Vacuum 84 (2010) 1280–1286.

[26] Chul-Hwan Choi, Seon-Hyo Kim, Effects of post-annealing temperature on structural, optical, and electrical properties of ZnO and $Zn_{1-x}Mg_xO$ films by reactive RF magnetron sputtering, Journal of Crystal Growth 283 (2005) 170–179.

[27] C. Xu, J. Tamaki, N. Miura, N. Yamazoe, Grain size effects on gas sensitivity of porous SnO_2-based elements, Sensors and Actuators, B—Chemicals 3 (1991) 147–155.

[28] Hye-Won Lim, HyeJin Jun, Myung-June Park, Hyo-Sik Kim, JongWook Bae, Kyoung-Su Ha, Ho-Jeong Chae, Ki-Won Jun, Optimization of methanol synthesis reaction on $Cu/ZnO/Al_2O_3/ZrO_2$ catalyst using genetic algorithm: maximization of the synergetic effect by the optimal CO_2 fraction, Korean Journal of Chemical Engineering 27 (6) (2010) 1760–1767.